

Global phase synchronization in an array of time-delay systems

R. Suresh^{1,*}, D. V. Senthilkumar^{2,3,†}, M. Lakshmanan^{1,‡} and J. Kurths^{3,4,§}

¹*Centre for Nonlinear Dynamics, Department of Physics,
Bharathidasan University, Tiruchirapalli-620024, India*

²*Centre for Dynamics of Complex Systems, University of Potsdam, 14469 Potsdam, Germany*

³*Potsdam Institute for Climate Impact Research, 14473 Potsdam, Germany*

⁴*Institute of Physics, Humboldt University, 12489 Berlin, Germany*

(Dated: February 15, 2022)

We report the identification of global phase synchronization (GPS) in a linear array of unidirectionally coupled Mackey-Glass time-delay systems exhibiting highly non-phase-coherent chaotic attractors with complex topological structure. In particular, we show that the dynamical organization of all the coupled time-delay systems in the array to form GPS is achieved by sequential synchronization as a function of the coupling strength. Further, the asynchronous ones in the array with respect to the main sequentially synchronized cluster organize themselves to form clusters before they achieve synchronization with the main cluster. We have confirmed these results by estimating instantaneous phases including phase difference, average phase, average frequency, frequency ratio and their differences from suitably transformed phase coherent attractors after using a nonlinear transformation of the original non-phase-coherent attractors. The results are further corroborated using two other independent approaches based on recurrence analysis and the concept of localized sets from the original non-phase-coherent attractors directly without explicitly introducing the measure of phase.

PACS numbers: 05.45.Xt, 05.45.Pq

I. INTRODUCTION

Chaotic phase synchronization (CPS), referred to as the locking of the phases of the coupled chaotically evolving dynamical systems, has been investigated in ensembles of globally coupled arrays [1–9, 11–13], networks of oscillators [14–17] with applications to electrochemistry [7, 8], laser systems [12, 13], cardiorespiratory systems [18–20], neuroscience [21–23], ecology [24–26], climatology [27–29], etc. Even though the notion of CPS is well studied in low dimensional systems, there exist very little indepth studies in higher dimensional systems such as time-delay systems which are essentially infinite-dimensional in nature and often exhibit high-dimensional, highly non-phase-coherent hyperchaotic attractors with complex topological structure. Consequently, estimating phase explicitly to identify phase synchronization in such systems is quite difficult. Nevertheless, CPS has been recently demonstrated in two coupled piecewise linear and Mackey-Glass time-delay systems [30, 31] by introducing a nonlinear transformation of the original dynamical variable to recast the original non-phase-coherent hyperchaotic attractors into smeared limit cycle-like attractors in order to facilitate the estimation of the phase variable using the available methods. However, these investigations are carried out so far only in two coupled time-delay systems. In view

of the widespread applications of CPS in ensembles of coupled oscillators, here we investigate the existence of global phase synchronization (GPS) in an array of unidirectionally coupled Mackey-Glass time-delay systems and analyse the mechanism behind the dynamical organization of the coupled oscillators to form GPS. At first, we use the nonlinear transformation introduced in [30, 31] to estimate explicitly the phases of all the oscillators in the array and identify the existence of GPS in the array. Further, the existence of GPS is also confirmed from the original non-phase-coherent chaotic attractors themselves using two independent approaches, namely recurrence analysis [32, 33] and the concept of localized sets [34].

In addition, we will show that the onset of GPS in such arrays does not happen instantaneously, but instead takes place as a form of sequential synchronization. For lower values of coupling strengths the phases of nearby systems get already synchronized with the drive system in contrast to the far away systems. This sequential synchronization of chaotic systems can have applications in communication systems [35]. Furthermore, other non-synchronized time-delay systems with respect to the sequentially synchronized cluster display clusters of phase synchronized states among themselves before they become synchronized with the large cluster in the sequence to form global phase synchronization. This clustering is observed when the group of oscillators splits into subgroups such that all the oscillators within one cluster move in perfect phase synchrony. This clustering is considered to be particularly significant in biological systems [36–38]. Recently cluster synchronization in an array of three chaotic lasers without delay was reported [39] as well. Also global synchronization via cluster formation

*Electronic address: suresh@cnld.bdu.ac.in

†Electronic address: skumar@cnld.bdu.ac.in

‡Electronic address: lakshman@cnld.bdu.ac.in

§Electronic address: juergen.kurths@pik-potsdam.de

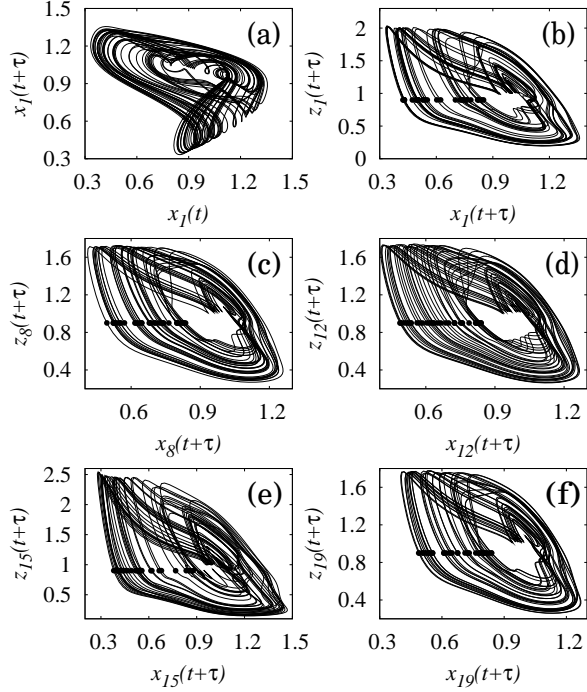


FIG. 1: (a) Non phase-coherent chaotic attractor of the drive system given by Eq. (1a). (b) Transformed attractor (using Eq. (2)) of the drive system. (c-f) Transformed attractors of some randomly selected response systems ($i = 8, 12, 15, 19$) in the projected phase space $(x_i(t + \tau), z_i(t + \tau))$, where they look like smeared limit cycle attractors in the absence of the coupling along with the Poincaré points represented by filled circles. Here τ has been chosen as $\tau = 20.0$.

has been observed in coupled phase oscillators without time-delay [10] with simultaneous phase slips of all oscillators, where quantized phase shifts in these phase slips have been observed. By increasing the coupling, a bifurcation tree from high-dimensional quasiperiodicity to chaos to quasiperiodicity and periodicity has also been found.

The remaining paper is organized as follows: In Sec. II, we will describe briefly the coupling configuration and the nature of chaotic attractors exhibited by the Mackey-Glass time-delay system. The existence of global phase synchronization from the transformed attractors is discussed in Sec. III, which is also confirmed from the original non-phase-coherent chaotic attractors using recurrence analysis and the concept of localized sets in Sec. IV. Finally, we summarize our results in Sec. V.

II. LINEAR ARRAY OF MACKEY-GLASS TIME-DELAY SYSTEMS

The Mackey-Glass time-delay system was originally deduced as a model for blood production in patients with leukemia [40], and it has been well studied in the lit-

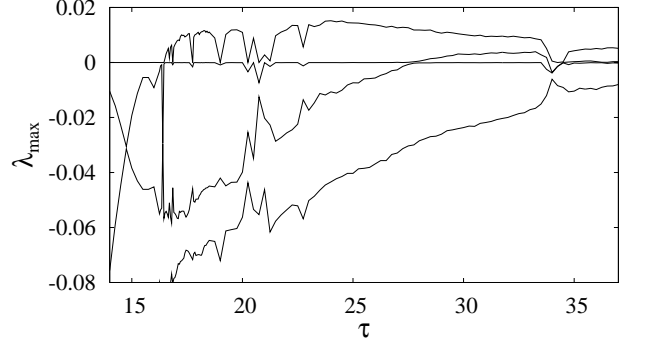


FIG. 2: The first four maximal Lyapunov exponents λ_{max} of the Mackey-Glass time-delay system (1a) for the parameter values $\alpha = 0.1, \beta = 0.2, \tau \in (14, 37)$ in the absence of the coupling C .

erature for its hyperchaotic behavior [41–43] and has also been experimentally realized using analog electronic circuits [44]. In this paper, we consider a linear array of unidirectionally coupled Mackey-Glass systems with free-end boundary conditions represented by the following system of coupled nonlinear first order ordinary differential equations,

$$\dot{x}_1(t) = -\beta x_1(t) + \frac{\alpha_1 x_1(t - \tau)}{(1 + x_1(t - \tau)^c)}, \quad (1a)$$

$$\dot{x}_i(t) = -\beta x_i(t) + \frac{\alpha_i x_i(t - \tau)}{(1 + x_i(t - \tau)^c)} + C(x_{i-1}(t) - x_i(t)), \quad i = 2, 3, \dots, N, (1b)$$

where, α, β, c are the system parameters, τ is the time-delay and C is the coupling strength. We have fixed the parameter values at $\alpha_1 = 0.2, \beta = 0.1, c = 10.0, \tau = 20.0$ and the values of the nonlinear parameter α_i of the response systems in the array are chosen randomly in the range $\alpha_i \in (0.17, 0.20)$, so that all the systems are effectively nonidentical. For our simulations, we have fixed the total number of oscillators in the array as $N = 20$, though we confirmed our results for $N = 50$ also (see Appendix A).

The uncoupled drive (1a) exhibits a highly non-phase-coherent chaotic attractor for the chosen parameter values, which is depicted in Fig. 1a. The first four largest Lyapunov exponents of the uncoupled drive system are shown in Fig. 2 as a function of the delay time τ . Note that the phase calculated directly from the original non-phase-coherent chaotic attractor (Fig. 1a) cannot yield monotonically increasing behaviour as it has several closed loops, which also contribute to the phase information, other than the main center of rotation of the major part of the trajectories [30, 31]. To overcome this problem a nonlinear transformation is introduced so as to rescale the original non-phase-coherent chaotic attractor into smeared limit cycle-like attractor with a single center of rotation. The transformation is performed by

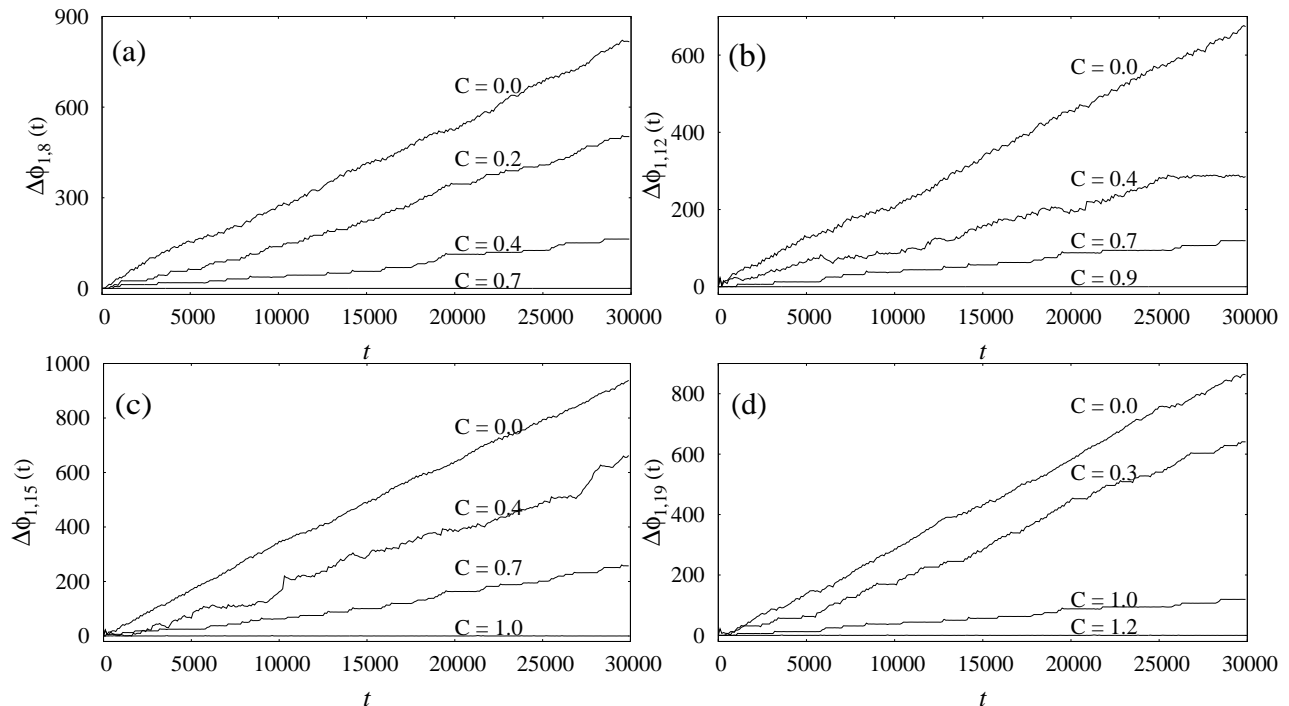


FIG. 3: (a-d) Phase differences ($\Delta\phi_{1,i} = \phi_1 - \phi_i$) of the randomly selected systems ($i = 8, 12, 15, 19$) from the array of coupled Mackey-Glass time-delay systems for different values of the coupling strength C . A more detailed description can be found in the text.

introducing a new state variable [30, 31],

$$z(t + \tau) = x(t)x(t + \hat{\tau})/x(t + \tau), \quad (2)$$

where $\hat{\tau}$ is the optimal value of time-delay to be chosen in order to avoid any additional center of rotation. This functional form of transformation (along with a delay time $\hat{\tau}$) has been identified by generalizing the transformation used in the case of chaotic attractors in the Lorenz systems [1]. Now, the projected trajectory in the new state space $(x(t + \tau), z(t + \tau))$ (Fig. 1b) resembles that of a smeared limit cycle-like attractor with a single fixed center of rotation. It is also to be noted that, even though the transformed attractor has sharp turns in the vicinity of the common center, it does not have any closed loops as in the original non-phase-coherent attractor. Otherwise, the transformed attractor would not give rise to monotonically increasing phase resulting in exact matching of the phases of the coupled time-delay systems [30, 31].

III. GPS FROM THE TRANSFORMED ATTRACTOR

In this section, we will show that the global phase synchronization in the array of Mackey-Glass time-delay systems (1) is attained by a sequential phase synchronization of the oscillators in the array as the coupling strength is

increased. Further we will also demonstrate that the remaining non-synchronized oscillators in the array form synchronized clusters among themselves before attaining GPS.

We use the same nonlinear transformation (2) to recast the original non-phase-coherent chaotic attractors of all the $N = 20$ oscillators into smeared limit cycle-like attractors. We have fixed the value of the optimal value $\hat{\tau}$ in Eq. (2) as $\hat{\tau} = 8.0$ for all the N oscillators. Instead one can also choose different values for $\hat{\tau}$ for different oscillators, as they are nonidentical systems with a parameter mismatch, to obtain more exact unfolding for different attractors. However, we find $\hat{\tau} = 8.0$ for all the oscillators is adequate for our purpose in the following study. We have calculated the instantaneous phases of all the oscillators using the Poincaré section technique [1, 2] from their corresponding transformed attractors. Projected trajectories of randomly selected response systems ($i = 8, 12, 15, 19$) in the array (1b) into the new state space $(x_i(t + \tau), z_i(t + \tau))$, where they look like smeared limit cycle-like attractors with a fixed center of rotation, are shown in Figs. 1(c-f). Filled circles in these plots correspond to the Poincaré points.

Phase differences, $\Delta\phi_i = \phi_1 - \phi_i$, between the drive and some randomly selected response systems ($i = 8, 12, 15, 19$) in the array (1b) are shown in Figs. 3 for different values of the coupling strength. They increase monotonically in the absence of coupling ($C = 0.0$) indicating that all the oscillators are in an asynchronous

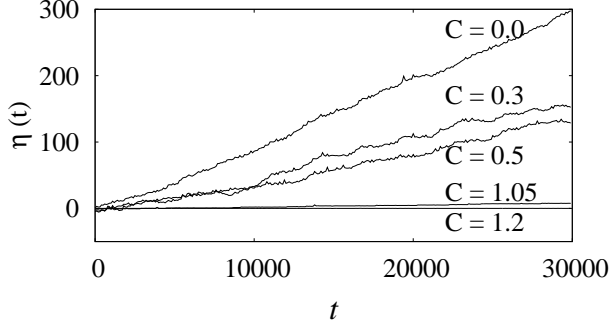


FIG. 4: The average phase difference ($\eta(t)$) for different values of the coupling strength C . For $C = 0.0$ the phases of all the systems are unbounded so the phase difference increases linearly with time but for $C = 1.2$ the phases of all the systems are bounded, showing a high quality phase synchronization.

state. Phase slips in the phase differences for small values of the coupling strength indicates that the oscillators are in the transition state to GPS. Further increase in the value of the coupling strength results in a strong boundedness of the phases of the oscillators. For sufficiently large C , the phase differences become zero (Figs. 3) indicating the existence of phase synchronization between the drive and the response systems. It is evident from the Figs. 3 that the 8th oscillator is synchronized with the drive at $C = 0.7$, while the other systems are in the transition state, whereas 12th oscillator is synchronized with drive only at $C = 0.9$. The other two oscillators with the index $i = 15$ and $i = 19$ reach synchronization with the drive for further larger values of the coupling strength, $C = 1.0$ and 1.2 , respectively. Therefore, it is clear that the nearby oscillators to the drive system in the array are synchronized first as the coupling strength is increased implying that the global phase synchronization is reached by sequential phase synchronization of the coupled oscillators in the array. To confirm the existence of GPS, we have calculated the average phase difference, $\eta(t)$, defined as

$$\eta(t) = \frac{1}{N-1} \sum_{j=2}^N (\phi_1 - \phi_j). \quad (3)$$

The average phase difference ($\eta(t)$) for different values C is shown in Fig. 4 as a function of time t . In the absence of the coupling ($C = 0.0$), the phases of all the oscillators evolve independently and hence their average phase difference increases linearly with time. Further increase in C induces the entrainment of phases of the oscillators and at the value of coupling strength $C = 1.2$ the average phase difference of all the N oscillators becomes exactly zero, showing a high quality GPS in the array.

The emergence of GPS through a sequential phase synchronization is also characterized by calculating the time averaged phase ($\langle \phi_i \rangle$) and the time averaged frequency

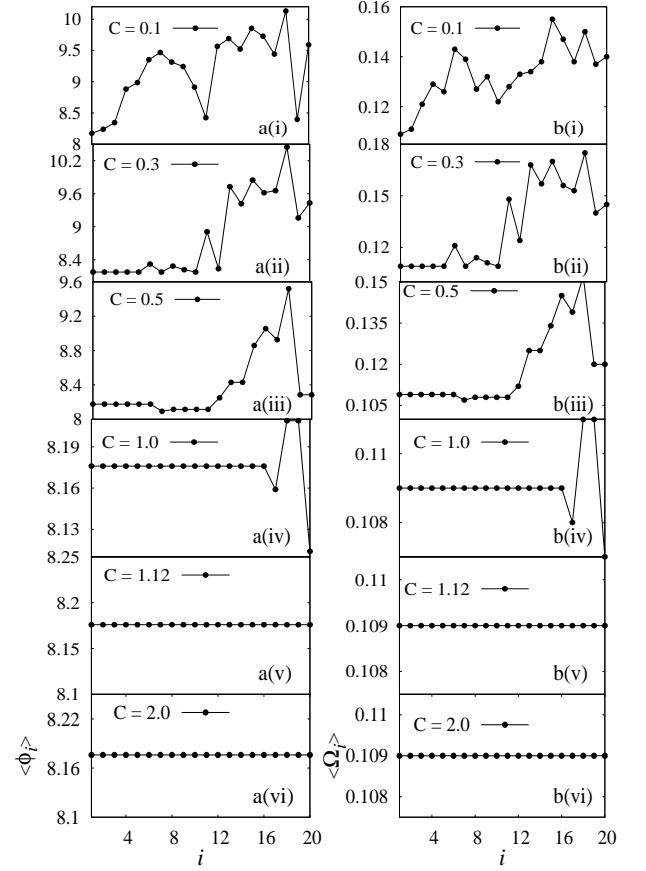


FIG. 5: (a) Time averaged phase ($\langle \phi_i \rangle$) and (b) time averaged frequency ($\langle \Omega_i \rangle$) of all the systems plotted as a function of the system index i for various values of the coupling strength C .

($\langle \Omega_i \rangle$) of each of the oscillators in the array which are defined as

$$\langle \phi_i(t) \rangle = \left\langle 2\pi k + 2\pi \frac{t^i - t_k^i}{t_{k+1}^i - t_k^i} \right\rangle_t, \quad (t_k^i < t^i < t_{k+1}^i) \quad (4a)$$

$$\langle \Omega_i(t) \rangle = \lim_{T \rightarrow \infty} \frac{1}{T} \int_0^T \dot{\phi}_i(t) dt, \quad (4b)$$

where t_k^i is the time of the k^{th} crossing of the flow with the Poincaré section of the i^{th} attractor and $\langle \dots \rangle_t$ denotes a time average. The average phase and the average frequency are shown in Figs. 5a and Figs. 5b, respectively, for different values of the coupling strength as a function of the oscillator index. A random distribution of the average phase (Fig. 5a(i)) and the average frequency (Fig. 5b(i)) for the value of the coupling strength $C = 0.1$ indicate that the coupled oscillators in the array evolve almost independently. A slight increase in the coupling strength (to $C = 0.3$) results in synchronous evolution of the first 5 oscillators in the array as seen in Fig. 5a(ii) and Fig. 5b(ii). For $C = 0.5$, Fig. 5a(iii) and Fig. 5b(iii) indicate that the first 6 oscillators are synchronized. It is also to be noted from these figures that the other desynchronized oscillators form synchronized clusters among

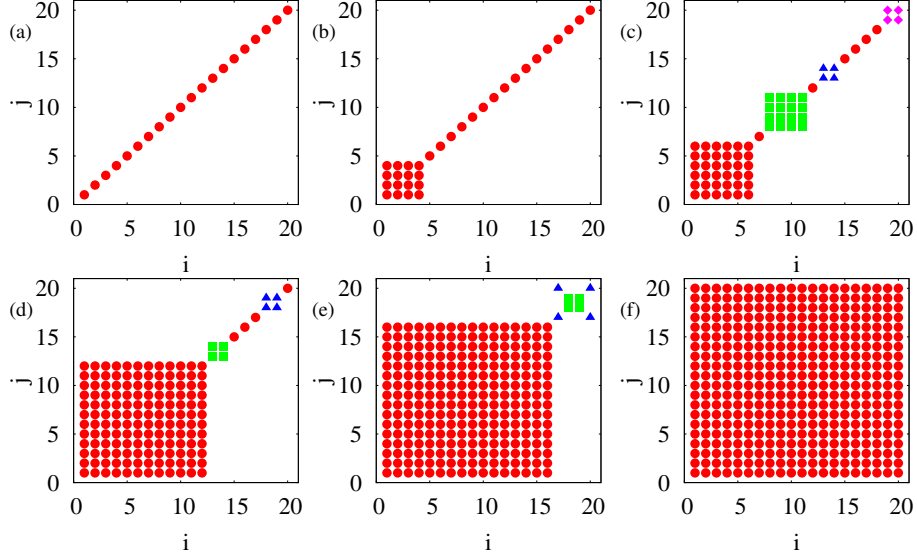


FIG. 6: (Colour online) Snap shots of the node vs node diagrams (that is oscillator index vs oscillator index plots) indicating the sequential phase synchronization and the organization of cluster states for different values of coupling strength. The different symbols indicate that the corresponding nodes are phase synchronized. (a) non phase synchronized case for $C = 0.1$ (b) First four oscillators in Eq. (1b) are phase synchronized with the drive system for $C = 0.27$. (c), (d) and (e) Sequential phase synchronization and the formation of small cluster states for $C = 0.5, 0.82$ and 1.08 , respectively, and (f) Global phase synchronization for $C = 1.2$.

themselves. In particular, the oscillators with the indices $8 - 11$ synchronize among themselves to form a cluster, while the oscillators with the indices $13 - 14$, and $19 - 20$ form separate small clusters. These clusters can also be clearly visualized by plotting the oscillator index plots as we will illustrate below. It is also to be noted that even when the total number of oscillators in the array is increased, the phenomenon remains qualitatively the same though the sizes of the clusters will increase appropriately (see Appendix A below for some details for $N = 50$). We also note that the results remain qualitatively unaltered even for different sets of random values for the nonlinear parameters, α_i , confirming the robustness of our results. A similar transition to PS through clustering, termed as hard transition for large coupling strength, in a chain of diffusively coupled Rössler oscillators with large frequency mismatch have been observed [9] but in the periodic state due to the suppression of chaotic attractors. For further larger values of the coupling strength, the desynchronized oscillators form similar small clusters among themselves before attaining GPS. The average phase and the average frequency illustrated in Fig. 5a(iv) and Fig. 5b(iv) for $C = 1.0$ indicates that most of the nearest oscillators are synchronized with the drive, while the oscillators with the indices $18 - 19$ form a small separate cluster. All the oscillators in the array become phase/frequency locked and evolve in synchrony (GPS) with each other for the coupling strength $C = 1.12$ as depicted in Fig. 5a(v) and Fig. 5b(v) and they continue to be in a stable phase/frequency synchronized state which

is shown in Fig. 5a(vi) and Fig. 5b(vi) for $C = 2.0$.

The mechanism for the formation of clusters and GPS may be explained as follows. Due to the mismatches in the nonlinear parameters, α_i , all the individual systems in the array evolve independently with different phases (phase mismatches), and correspondingly with frequency mismatches, for small values of the coupling strength C . As C is increased further, the oscillators with nearest frequencies in the array synchronize first to form clusters among themselves leaving the clusters with relatively large frequency mismatch in isolation (see Figs. 6 and 13). Further increase in C results in the formation of a single large cluster whose constituents exhibit a coherent phase oscillation with the drive due to the decomposition of the clusters away from the drive in the array. Consequently GPS results in the system. Similar mechanism has been identified in ensemble of coupled Rössler oscillators with frequency mismatches [45] (without time-delay).

The above dynamical organization of GPS via sequential phase synchronization and the clustering can be also be visualized clearly by using snap shots of the oscillators in the index vs index plot, as node vs node diagrams, as shown in Fig. 6. The oscillators that evolve with identical values of the average phase/frequency are assigned with identical shapes. The diagonal line in Fig. 6a for $C = 0.1$ corresponds to the oscillator index $i = j$ and they evolve independently. Figure 6b indicates that the first four oscillators in the array are synchronized with the drive for $C = 0.27$. As discussed above, three small clusters are seen in Fig. 6c for $C = 0.5$ while the first 6 oscillators

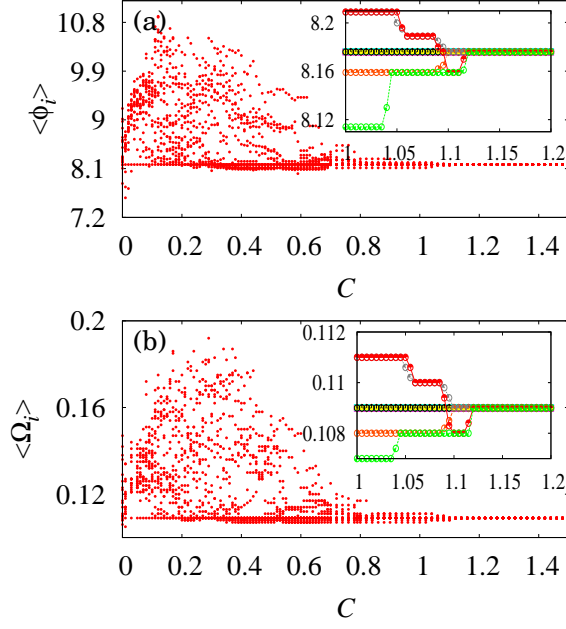


FIG. 7: (Colour online) (a) Time averaged phase ($\langle \phi_i \rangle$) and (b) Time averaged frequency ($\langle \Omega_i \rangle$), $i = 1, 2, \dots, 20$ plotted as a function of the coupling strength $C \in (0, 1.5)$. Here for each value of C we have plotted the average phase/frequency of all the $N = 20$ oscillators which is shown by the filled circles. Insets show some of the systems get synchronized themselves to form small clusters (each subgroup of oscillator is differentiated by different types of circles) before they synchronize with the drive system to form GPS.

form a large synchronized cluster. Similar small clusters are shown in Figs. 6d and 6e for $C = 0.82$ and 1.08 , respectively, in addition to the single large cluster formed by sequential phase synchronization of the oscillators in the array. Finally, GPS of all the oscillators in the array is illustrated in Fig. 6f for $C = 1.2$.

For a global picture of the emergence of GPS, we have plotted the average phase ($\langle \phi_i \rangle$) and the average frequency ($\langle \Omega_i \rangle$) of all the N oscillators as a function of the coupling strength C in Figs. 7. There is an absence of any correlation among the average phases (Fig. 7a) and the average frequencies (Fig. 7b) of different oscillators for low values of the coupling strength as revealed by the random distributions of their values. The random distribution of $\langle \phi_i \rangle$ and $\langle \Omega_i \rangle$ are organized into few clusters for $C \geq 0.5$ as may be evident from the Figs. 7. Global phase synchronization emerges for $C \geq 1.12$ as may be seen from the insets. Small synchronized clusters formed by the remaining asynchronous oscillators for larger values of C can also be appreciated from the insets.

We have also plotted the frequency difference ($\Delta\Omega_{1,j}$, $j = 2, 3, \dots, N$) and the frequency ratio (Ω_j/Ω_1 , $j = 2, 3, \dots, N$) of all the oscillators with that of the drive as a function of the coupling strength by different types of lines in Fig. 8a and Fig. 8b, respectively.

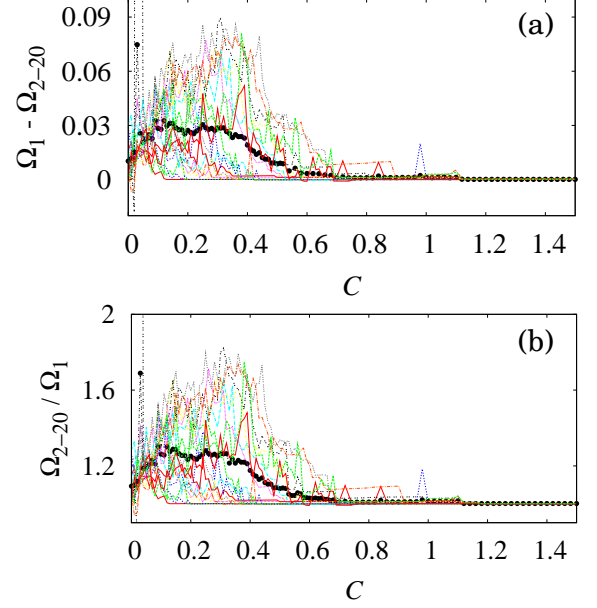


FIG. 8: (Colour online) (a) The frequency difference ($\Delta\Omega_{1,j}$, $j = 2, 3, \dots, N$) and (b) the frequency ratio (Ω_j/Ω_1 , $j = 2, 3, \dots, N$) are plotted as a function of the coupling strength $C \in (0, 1.5)$. Each line corresponds to the difference/ratio between a response system and the drive system. The black filled circles indicate the average frequency difference/ratio of all the $(N - 1)$ response systems from the drive system.

The black filled circles in Fig. 8a and Fig. 8b correspond to the average frequency difference and the average frequency ratio of all the oscillators with that of the drive. The substantial saturation in their values for $C \geq 1.12$ indicates the emergence of GPS.

The emergence of global phase synchronization in the array can also be quantified using the well-known order parameter [47],

$$R e^{i\psi} = \left\langle \left| \frac{1}{N} \sum_{j=1}^N e^{i\phi_j(t)} \right| \right\rangle_t \quad (5)$$

where $\phi_j(t)$ denotes the instantaneous phase of the j^{th} system, $\psi(t)$ is the average phase and $\langle \dots \rangle_t$ denotes a time average. If all the systems are in a phase synchronized state then $R \approx 1$. The order parameter (R) is plotted in Fig. 9 for the number of oscillators $N = 20$ and $N = 50$ as a function of the coupling strength C . As C is increased, R also increases and for $N = 20$ the critical value of the coupling is $C > 1.12$ and for $N = 50$, C will be > 2.4 , for the value of $R \approx 1$ confirms the existence of GPS in the array of coupled time-delay systems.

IV. GPS FROM THE ORIGINAL NON-PHASE-COHERENT ATTRACTOR

In this section, we demonstrate the existence of GPS from the original non-phase-coherent chaotic attractors using two different approaches, namely recurrence quantification analysis [32, 33] and the concept of localized sets [34] without estimating explicitly the measure of phase.

A. GPS using recurrence analysis

Several measures of complexity which quantify small scale structures in the recurrence plots have been proposed and are known as recurrence quantification analysis (RQA) [32, 33]. Certain measures have also been introduced to characterize and identify different kinds of synchronization transitions in coupled chaotic systems. These measures have the advantage of applicability in the analysis of experimental systems and, in particular, in the case of very small available data sets. Further, these measures can also be used in the case of non-phase-coherent chaotic/hyperchaotic attractors of time-delay systems [30, 31, 46], where it is difficult and often even impossible to calculate the phase explicitly. Among the available recurrence quantification measures, we use the Correlation of Probability of Recurrence (CPR) and the generalized autocorrelation function $P(t)$ to confirm the existence of GPS in the array of coupled time-delay systems (1), both qualitatively and quantitatively.

A criterion to quantify phase synchronization between two systems is the Correlation of Probability of Recurrence (CPR) defined as

$$CPR = \langle \bar{P}_1(t) \bar{P}_2(t) \rangle / \sigma_1 \sigma_2, \quad (6)$$

where $P(t)$ is the generalized autocorrelation function represented as

$$P(t) = \frac{1}{N-t} \sum_{i=1}^{N-t} \Theta(\epsilon - \|X_i - X_{i+t}\|), \quad (7)$$

where Θ is the Heaviside function, X_i is the i^{th} data point of the system X , ϵ is a predefined threshold, $\|\cdot\|$ is the Euclidean norm, and N is the number of data points, $\bar{P}_{1,2}$ means that the mean value has been subtracted and $\sigma_{1,2}$ are the standard deviations of $P_1(t)$ and $P_2(t)$, respectively. Looking at the coincidence of the positions of the maxima of $P(t)$ of the systems, one can qualitatively identify PS [32, 33]. If both systems are in CPS, the probability of recurrence is maximal at the same time t and $CPR \approx 1$. If they are not in CPS, the maxima do not occur simultaneously and hence one can expect a drift in both the probability of recurrences resulting in low values of CPR.

The generalized autocorrelation function of the drive $P_1(t)$ and that of some response systems ($i = 8, 12$, and

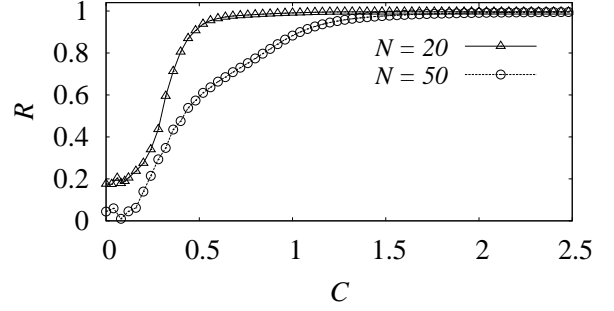


FIG. 9: The phase order parameter (R) for the number of oscillators $N = 20$ and $N = 50$ as a function of the coupling strength indicating global phase synchronization in the array of coupled Mackey-Glass time-delay systems.

19) $P_8(t)$, $P_{12}(t)$, and $P_{19}(t)$ are depicted in Fig. 10 for different values of the coupling strength. In the absence of coupling ($C = 0.0$), all systems evolve independently and hence the maxima of their respective generalized autocorrelation functions do not occur simultaneously as shown in Fig. 10a. On increasing the coupling strength, oscillators with a lower value of index in the array become synchronized first resulting in sequential phase synchronization and this can also be identified from the generalized autocorrelation functions of the response systems in the array. For instance, $P_8(t)$, $P_{12}(t)$, and $P_{19}(t)$ are shown along with $P_1(t)$ in Fig. 10b for $C = 0.4$. It is clear from this figure that the maxima of the drive $P_1(t)$ and those of the response $P_8(t)$ are in complete agreement with each other (Fig. 10bi) indicating the existence of PS between them. On the other hand, only some of the maxima of the response system $P_{12}(t)$ are in coincidence with those of the drive (Fig. 10bii) illustrating that the response system $i = 12$ is in transition to PS, whereas the maxima of the response system $P_{19}(t)$ do not coincide with those of the drive (Fig. 10biii) indicating that the response system $i = 19$ is in an asynchronous state for the same value of C . For $C = 1.2$, almost all of the positions of the peaks of the generalized auto correlation functions $P_1(t)$, $P_8(t)$, $P_{12}(t)$, and $P_{19}(t)$ are in agreement with each other as illustrated in Fig. 10(c) confirming the existence of GPS via sequential phase synchronization. It is also to be noted that the magnitudes of the peaks of all the oscillators have generally of different values and the differences in the heights of the peaks indicate that there is no correlation in the amplitudes of the coupled systems. Furthermore, the formation of clusters by the other asynchronous oscillators in the array can also be realized by plotting their respective generalized autocorrelation functions, which will show that all their maxima are in good agreement with each other, whereas there exists a drift between them and the maxima of the sequentially synchronized cluster.

The existence of GPS via sequential phase synchronization is also quantified using value of the index CPR of the

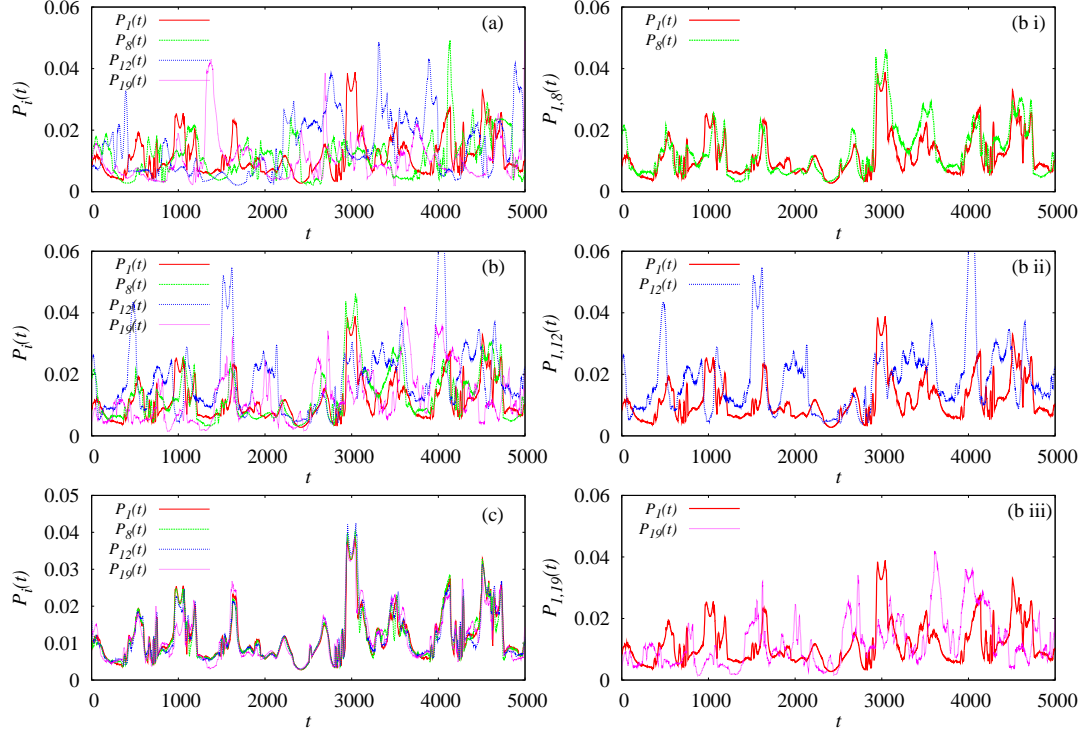


FIG. 10: (Colour online) Generalized autocorrelation functions of the drive $P_1(t)$ and randomly selected response systems ($i = 8, 12, \text{and } 19$) $P_8(t)$, $P_{12}(t)$, and $P_{19}(t)$ indicating (a) Non-phase-synchronization for $C = 0.0$, (b) generalized autocorrelation functions for $C = 0.4$ (bi) PS between the systems 1 and 8, (bii) approximate PS between the systems 1 and 12 and (biii) non PS between the systems 1 and 19, and (c) PS between all the systems ($i = 1, 8, 12$, and 19) for $C = 1.2$.

response systems with the drive as shown in Fig. 11. The different lines correspond to the index of the oscillators ($i = 2, 8, 12, 19$) in the array. It is evident from the figure that the oscillators with increasing index attain the value of unity in a sequence as a function of the coupling strength and finally for $C > 1.12$ the CPR of all the response systems with the drive reaches unity confirming that all the coupled oscillators are in GPS. The mean value of CPR of all the response systems in the array is shown as filled circles, which also confirms the existence of GPS for $C > 1.12$.

B. GPS using the concept of localized sets

Recently, an interesting framework to identify CPS, namely, the concept of localized sets [34] has been introduced. This approach provides an easy and efficient way to detect CPS especially in complicated non-phase-coherent attractors. The basic idea of this concept is to define a typical event in one of the systems and then observe the other system whenever this event occurs. These observations give rise to a set D . Depending upon the property of this set D , one can state whether PS exists or not. The coupled systems evolve independently if the sets obtained by observing the corresponding events in the systems spread over the attractor of the systems. On

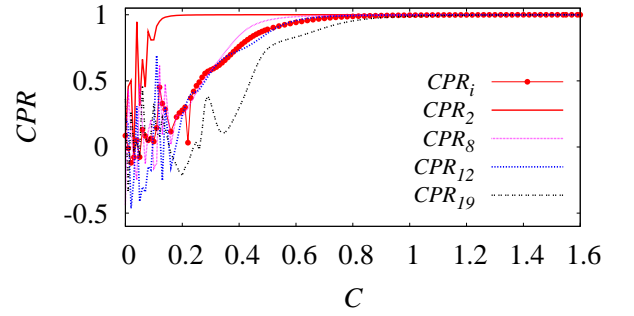


FIG. 11: (Colour online) The index CPR as a function of the coupling strength C . Different lines correspond to the CPR of different ($i = 2, 8, 12$, and 19) response systems with the drive system. The filled circles correspond to the mean value of the CPR of all the $(N - 1)$ systems in the array.

the other hand, if the sets are localized on the attractors then CPS exists between them.

We have confirmed the existence of the GPS in the linear array of Mackey-Glass time-delay systems (1) by using this concept of localized sets. Now, we will demonstrate the existence of GPS via sequential phase synchronization in the randomly selected response systems ($i = 1, 8, 12, 19$). We have defined the event as Poincaré sec-

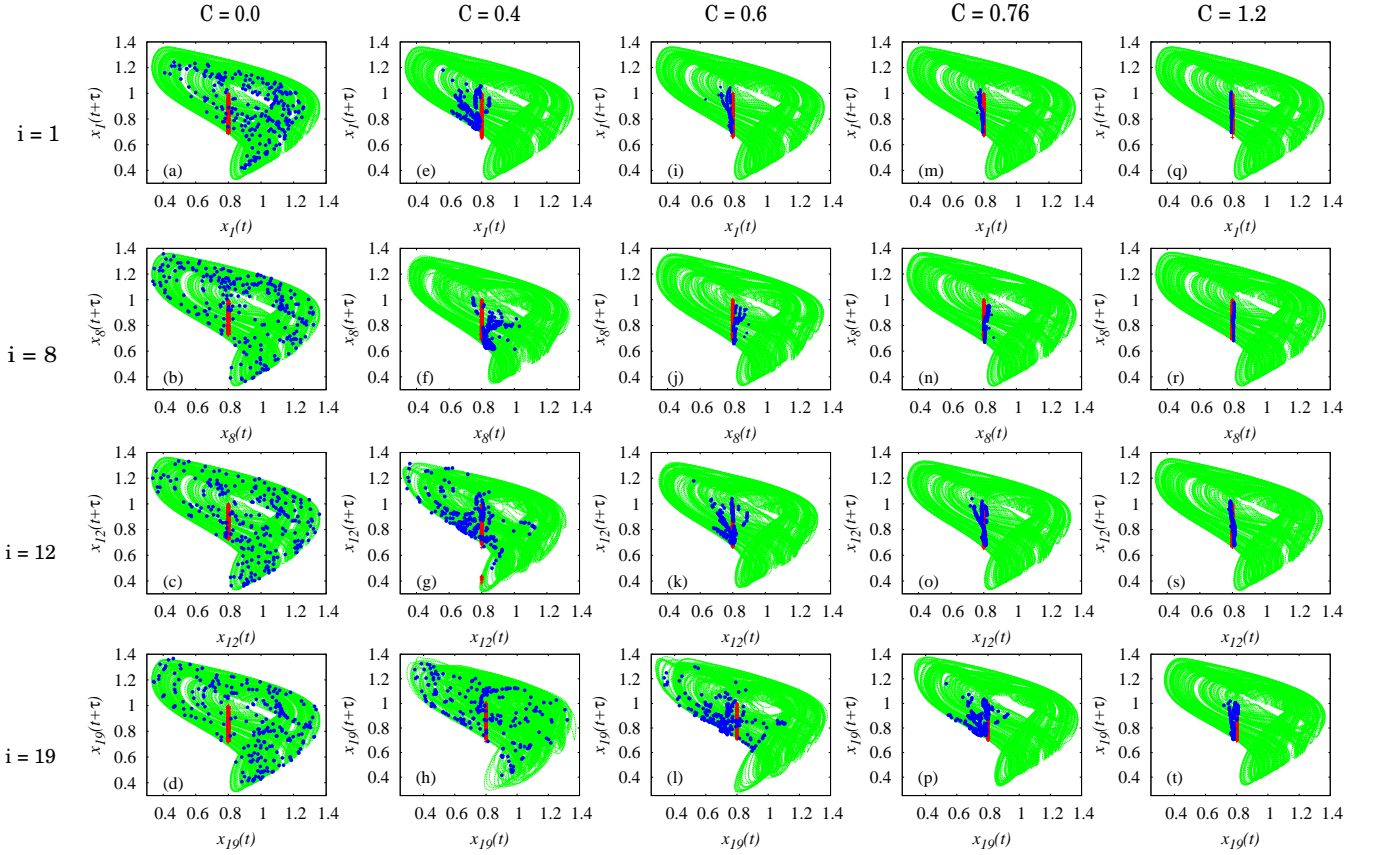


FIG. 12: (Colour online) First row (a-q) corresponds to the attractors of the drive system ($i = 1$) and the rows (b-r, c-s, and d-t) correspond to the attractors of some randomly selected response systems ($i = 8, 12, 19$). The ‘+’ marks represent the events (Poincaré sections) in the corresponding attractors. In (a-d) the sets (represented by the filled circles) are spread over the attractors and hence there is no CPS for the value of coupling strength $C = 0.0$. In (e-h) for $C = 0.4$ and in (i-l, m-p, q-t) the sets are localized confirming the existence of GPS in the array for $C = 0.6, 0.76$, and 1.2 , respectively.

tions in the attractors indicated as ‘+’ marks in Figs. 12. The set, indicated as filled circles, obtained by observing the drive system ($i = 1$) whenever the defined event occurs in the response system ($i = 8$) is shown in Fig. 12 (a) and that obtained by observing the response systems $i = 8, 12, 19$ whenever the defined event occurs in the drive system are shown in Figs. 12 (b-d) for the value of coupling strength $C = 0.0$. As the obtained sets are spread over the attractors, all the systems evolve independently and there is no CPS in the absence of coupling between them. Further when we increase the coupling strength to $C = 0.4$, the oscillator ($i = 8$) is partially synchronized with the drive as the sets are almost localized but the sets in the oscillators $i = 12, 19$ are spread over the attractors which means that they are not yet phase synchronized with the drive system. This is shown in Figs. 12 (e-h). Again increasing the coupling strength to $C = 0.6$, the sets are further bounded to a small region over the attractors which shows that the oscillators $i = 8, 12$ are synchronized with the drive, but the oscillator $i = 19$ is less phase synchronized with the drive which is represented by the spread of the events over the attractor

as shown in Figs. 12 (i-l). Further, the Figs. 12 (m-p) and Figs. 12 (q-t) indicate the situation for $C = 0.76$ and $C = 1.2$, respectively, where all the oscillators are now phase synchronized with the drive as the sets are localized over the attractor confirming the existence of GPS in an array via sequential phase synchronization as the coupling strength is increased.

Further, the formation of clusters can also be realized using the concept of localized sets by defining the event among the response systems that form the clusters and observing the other response systems that are in the same cluster. In this case the obtained sets by observing the event in the drive will spread over the attractor of the response systems, while the sets obtained by observing the event among the response systems that form a cluster will be localized on their respective attractors.

V. SUMMARY AND CONCLUSION

We have demonstrated the existence of global phase synchronization via sequential phase synchronization

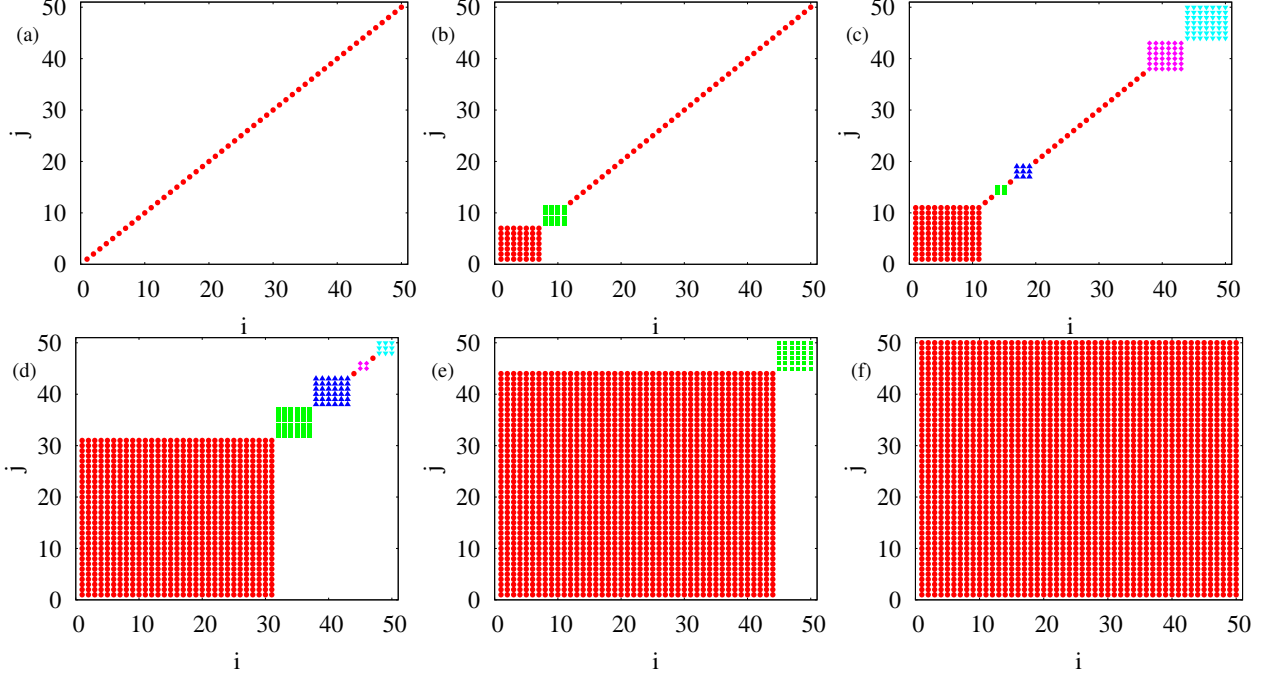


FIG. 13: (Colour online) Snap shots of the node vs node diagram indicating the sequential phase synchronization and the organization of cluster states of $N = 50$ oscillators for different values of coupling strength, C . The different symbols indicate that the corresponding nodes are phase synchronized. (a) Non-phase synchronized case for $C = 0.1$, (b) First seven oscillators in Eq. (1b) are phase synchronized with the drive system for $C = 0.4$, (c), (d) and (e) Sequential phase synchronization and the formation of small cluster states for $C = 0.53$, 1.9 and 2.3 , respectively, and (f) Global phase synchronization of $N = 50$ oscillators for $C = 2.5$.

in an array of coupled Mackey-Glass time-delay systems with parameter mismatches, which exhibit highly non-phase-coherent attractors with complex topological structure. Further, we have also shown that the remaining asynchronous systems will organize themselves to form different clusters before they get phase synchronized with the main cluster to form global phase synchronization. We have confirmed the existence of GPS via sequential phase synchronization by estimating the phase difference as a function of the coupling strength, the average frequency and the average phase as a function of the oscillator index and the coupling strength after calculating the phase variables from the transformed attractors. We have also demonstrated the existence of sequential phase synchronization and the formation of clusters by the remaining oscillators using the average frequency, average phase and specifically using the index vs index plot of the oscillators. Furthermore, we have also confirmed the existence of GPS via sequential phase synchronization using the recurrence quantification measures and the concept of localized sets which are calculated from the original non-phase-coherent attractors of the coupled Mackey-Glass time-delay systems. It is also to be noted that we have obtained similar transitions to GPS via clustering even in the hyperchaotic regimes of Fig. 2 for the Mackey-Glass systems and also in the coupled piecewise linear time-delay systems (with five positive Lyapunov

exponents).

Acknowledgments

The work of R.S. and M.L. has been supported by the Department of Science and Technology (DST), Government of India sponsored IRHPA research project, and DST Ramanna program of M.L. D.V.S. has been supported by the Alexander von Humboldt Foundation. J.K. acknowledges the support from EU under project No. 240763 PHOCUS(FP7-ICT-2009-C).

Appendix A:

The dynamical organization of GPS via sequential phase synchronization and the cluster formation can be visualized by using the snap shots of $N = 50$ oscillators in the index vs index plot as shown in Fig.13. The diagonal line in Fig.13 (a) for the value of coupling $C = 0.1$ corresponds to the oscillator index $i = j$ and the oscillators evolve independently. Further in Fig.13 (b), the first seven oscillators in the array are synchronized with the drive and the oscillators 8–11 form a separate cluster for the coupling strength $C = 0.4$. Further, the first eleven

oscillators in the array are synchronized and four small separate clusters are seen in Fig.13 (c) for $C = 0.53$. Similar small clusters are formed in Fig.13 (d) for $C = 1.9$ while the first thirty one oscillators form a large synchronized cluster. Further, in Fig.13 (e) the first forty four

oscillators are synchronized with the drive and the oscillators 45–50 form a separate cluster for $C = 2.3$. Finally, the occurrence of GPS of all the oscillators in the array is illustrated in Fig.13 (f) for the value of coupling strength $C = 2.5$.

-
- [1] A. S. Pikovsky, M. G. Rosenblum, and J. Kurths, *Synchronization - A Unified Approach to Nonlinear Science* (Cambridge University Press, Cambridge, 2001).
 - [2] S. Boccaletti, J. Kurths, G. Osipov, D. L. Valladares, and C. S. Zhou, Phys. Rep. **366**, 1 (2002).
 - [3] Int. J. Bifurcation Chaos Appl. Sci. Eng. **10** (2000), special issue on Phase synchronization edited by J. Kurths.
 - [4] M. V. Ivanchenko, G. V. Osipov, V. D. Shalfeev, and J. Kurths, Phys. Rev. Lett. **93**, 134101 (2004).
 - [5] A. Takamatsu, T. Fujii, and I. Endo, Phys. Rev. Lett. **85**, 2026 (2000).
 - [6] A. S. Pikovsky, M. G. Rosenblum, and J. Kurths, Europhys. Lett. **34**, 165 (1996).
 - [7] I. Z. Kiss, Y. Zhai, and J. L. Hudson, Phys. Rev. Lett. **88**, 238301 (2002).
 - [8] C. Zhou, J. Kurths, I. Z. Kiss, and J. L. Hudson, Phys. Rev. Lett. **89**, 014101 (2002).
 - [9] G. V. Osipov, A. S. Pikovsky, M. G. Rosenblum, and J. Kurths, Phys. Rev. E **55**, 2353 (1997).
 - [10] Z. Zheng, G. Hu, and B. Hu, Phys. Rev. Lett. **81**, 5318 (1998).
 - [11] M. Zhan, Z. G. Zheng, G. Hu, and Xi-hong Peng, Phys. Rev. E **62**, 3552 (2000).
 - [12] G. Kozyreff, A. G. Vladimirov, and P. Mandel, Phys. Rev. Lett. **85**, 3809 (2000).
 - [13] K. Otsuka, Y. Miyasaka, T. Narita, S. C. Chu, C. C. Lin, and J. Y. Ko, Phys. Rev. Lett. **97**, 213901 (2006).
 - [14] S. Boccaletti, V. Latora, Y. Moreno, M. Chavez, and D. U. Hwang, Phys. Rep. **424**, 175 (2006).
 - [15] A. Arenas, A. Daz-Guilera, J. Kurths, Y. Moreno, and C. Zhou, Phys. Rep. **469**, 93 (2008).
 - [16] C. A. S. Batista, A. M. Batista, J. A. C. dePontes, R. L. Viana, and S. R. Lopes, Phys. Rev. E **76**, 016218 (2007).
 - [17] Q. Ren, and J. Zhao, Phys. Rev. E **76**, 016207 (2007); X. Yu, Q. Ren, J. Hou, and J. Zhao, Phys. Lett. A **373**, 1276 (2009).
 - [18] C. Schäfer, M. G. Rosenblum, J. Kurths, and H.-H. Abel, Nature(London) **392**, 239 (1998).
 - [19] A. Stefanovska, H. Haken, P. V. E. McClintock, M. Hozic, F. Bajrovic, and S. Ribaric, Phys. Rev. Lett. **85**, 4831 (2000).
 - [20] R. Bartsch, J. W. Kantelhardt, T. Penzel, and S. Havlin, Phys. Rev. Lett. **98**, 054102 (2007).
 - [21] F. Varela, J. P. Lachaux, E. Rodriguez, and J. Martinerie, Neuroscience (Nature Reviews) **2**, 229 (2001).
 - [22] J. Lian, J. Shuai, and D. M. Durand, J. Neural Eng. **1**, 46 (2004).
 - [23] P. Tass, M. G. Rosenblum, J. Weule, J. Kurths, A. Pikovsky, J. Volkmann, A. Schnitzler, and H. -J. Freund, Phys. Rev. Lett. **81**, 3291 (1998).
 - [24] B. Blasius, A. Huppert, and L. Stone, Nature **399**, 354 (1999).
 - [25] E. Sismundo, Science **249**, 55 (1990).
 - [26] R. E. Amritkar, and G. Rangarajan, Phys. Rev. Lett. **96**, 258102 (2006).
 - [27] D. Rybski, S. Harlin, and A. Bunde, Physica A **320**, 601 (2003).
 - [28] K. Yamasaki, A. Gozolchiani, and S. Harlin, Prog. Theor. Phys. **179**, 178 (2009).
 - [29] D. Maraun, and J. Kurths, Geophys. Res. Lett. **32**, L15709 (2005).
 - [30] D. V. Senthilkumar, M. Lakshmanan, and J. Kurths, Phys. Rev. E **74**, 035205(R) (2006).
 - [31] D. V. Senthilkumar, M. Lakshmanan, and J. Kurths, Chaos **18**, 023118 (2008).
 - [32] M. C. Romano, M. Thiel, J. Kurths, I. Z. Kiss, and J. L. Hudson, Europhys. Lett. **71**, 466 (2005).
 - [33] N. Marwan, M. C. Romano, M. Thiel, and J. Kurths, Phys. Rep. **438**, 237 (2007).
 - [34] T. Pereira, M. S. Baptista, and J. Kurths, Phys. Rev. E **75**, 026216 (2007).
 - [35] Chil-Min Kim, S. Rim, and W-H. Kye, Phys. Rev. Lett. **88**, 014103 (2001).
 - [36] K. Kaneko, Physica D **41**, 137 (1990).
 - [37] A. Sherman, Bull. Math. Biol. **56**, 811 (1994).
 - [38] S. H. Strogatz, and I. Stewart, Sci. Am. **269**, 102 (1993).
 - [39] J. R. Terry, K. S. Thornburg, Jr., D. J. DeShazer, G. D. Vanwiggeren, S. Zhu, P. Ashwin, and R. Roy, Phys. Rev. E **59**, 4036 (1999).
 - [40] M. C. Mackey, and L. Glass, Science **197**, 287 (1977).
 - [41] C. Zhou, and C. H. Lai, Phys. Rev. E **60**, 320 (1999).
 - [42] K. Pyragas, Phys. Rev. E **58**, 3067 (1998).
 - [43] I. G. Szendro, and J. M. Lopez, Phys. Rev. E **71**, 055203 (2005).
 - [44] A. Namajūnas, and K. Pyragas, and A. Tamaševičius, Phys. Lett. A **201**, 42 (1995).
 - [45] G. V. Osipov, C. Zhou, and J. Kurths, *Synchronization in Oscillatory Networks* (Springer, Berlin, 2007).
 - [46] D. V. Senthilkumar, M. Lakshmanan, and J. Kurths, Eur. Phys. J. Special Topics **164**, 35 (2008).
 - [47] Y. Moreno, and A. F. Pacheco, Europhys. Lett. **68**, 603 (2004).